Title	Pterosaur integumentary structures with complex feather-like branching
Authors	Yang, Zixiao;Jiang, Baoyu;McNamara, Maria E.;Kearns, Stuart L.;Pittman, Michael;Kaye, Thomas G.;Orr, Patrick J.;Xu, Xing;Benton, Michael J.
Publication date	2018-12-17
Original Citation	Yang, Z., Jiang, B., McNamara, M. E., Kearns, S. L., Pittman, M., Kaye, T. G., Orr, P. J., Xu, X. and Benton, M. J. (2019) 'Pterosaur integumentary structures with complex feather-like branching', Nature Ecology & Evolution, 3(1), pp. 24-30. doi: 10.1038/s41559-018-0728-7
Type of publication	Article (peer-reviewed)
Link to publisher's version	https://www.nature.com/articles/s41559-018-0728-7 - 10.1038/s41559-018-0728-7
Rights	© 2019 Springer Nature Publishing AG. This is a post-peer-review, pre-copyedit version of an article published in Nature Ecology & Evolution. The final authenticated version is available online at: https://doi.org/10.1038/s41559-018-0728-7
Download date	2024-04-19 01:41:07
Item downloaded from	https://hdl.handle.net/10468/8311

1   **Pterosaur integumentary structures with complex feather-like branching**

2   Zixiao Yang[1], Baoyu Jiang[1], Maria E. McNamara[2], Stuart L. Kearns[3], Michael

3   Pittman[4], Thomas G. Kaye[5], Patrick J. Orr[6], Xing Xu[7], Michael J. Benton[3]

4

5   1. Center for Research and Education on Biological Evolution and Environments,

6   School of Earth Sciences and Engineering, Nanjing University, Nanjing 210023,

7   China

8   2. School of Biological, Earth and Environmental Sciences, University College Cork,

9   Cork T23 TK30, Ireland

10   3. Department of Earth Sciences, University of Bristol, Bristol BS8 1RJ, UK

11   4. Vertebrate Palaeontology Laboratory, Department of Earth Sciences, University of

12   Hong Kong, Pokfulam, Hong Kong, China

13   5. Foundation for Scientific Advancement, Sierra Vista, Arizona USA

14   6. UCD School of Earth Sciences, University College Dublin, Belfield, Dublin 4

15   D04V1W8, Ireland

16   7. Key Laboratory of Vertebrate Evolution and Human Origins, Institute of Vertebrate

17   Paleontology and Paleoanthropology, Chinese Academy of Sciences, Beijing 100044,

18   China

19

20   **Pterosaurs were the first vertebrates to achieve true flapping flight, but in the**

21   **absence of living representatives, many questions concerning their biology and**

22   **lifestyle remain unresolved. Pycnofibres, the integumentary coverings of**

23   **pterosaurs, are particularly enigmatic: although many reconstructions depict**

24   **fur-like coverings composed of pycnofibres, their affinities and function are not**

25   **fully understood. Here we report the preservation in two anurognathid pterosaur**

26   **specimens of morphologically diverse pycnofibres that show diagnostic features**

27   **of feathers, including non-vaned grouped filaments and bilaterally branched**

28   **filaments, hitherto considered unique to maniraptoran dinosaurs, and preserved**

29   **melanosomes with diverse geometries. These findings could imply that feathers**

30   **had deep evolutionary origins in ancestral archosaurs, or that these structures**

31   **arose independently in pterosaurs. The presence of feather-like structures**

32   **suggests that anurognathids, and potentially other pterosaurs, possessed a dense**

33   **filamentous covering that likely functioned in thermoregulation, tactile sensing,**

34   **signalling, and aerodynamics.**

35   Feathers are the most complex integumentary appendages in vertebrates[1]. Most

36   feathers in modern birds possess an axial shaft from which branch lateral barbs and

37   barbules. Much is known about the anatomy, developmental biology, and genomic

38   regulation of these structures, but their deep evolutionary origin is controversial[2-4].

39   Feathers and feather-like integumentary structures have been reported in many

40   theropod dinosaurs (including birds)[3,5] and ornithischians such as *Psittacosaurus*[6],

41   *Tianyulong*[7], and *Kulindadromeus*[8]. Feather-like or hair-like structures, termed

42   pycnofibres[9], have also been reported in several pterosaur specimens[9-13], but their

43   nature is not resolved.

44   Here we report remarkably well-preserved pycnofibres in two anurognathid

45   pterosaurs and demonstrate, using evidence from morphology, chemistry and

46   macroevolutionary analyses, that the preserved pycnofibres bear key features of

47   feathers: monofilaments, two types of non-vaned grouped filaments, bilaterally

48   branched filaments that were previously considered unique to maniraptoran dinosaurs,

49   and preserved melanosomes with diverse geometries. Both specimens studied are

50   from the Middle–Late Jurassic Yanliao Biota (ca. 165–160 Mya[14]). NJU–57003

51   (Nanjing University) is a newly excavated specimen from the Mutoudeng locality and

52   CAGS–Z070 (Institute of Geology, Chinese Academy of Geological Sciences), which

53   has been noted briefly for its feather-like branched pycnofibres[13], is from the

54   Daohugou locality. Both specimens are near-complete and well-articulated, with

55   extensive soft tissues (Figs. 1 and 2, and Supplementary Figs. 1–5). Both specimens

56   are identified as anurognathids[17] (see Supplementary text for osteological

57   descriptions).

58   Preserved soft tissues include structural fibres (actinofibrils) and pycnofibres.

59   Structural fibres, common in the pterosaur wing membrane[9,12,18], are observed only in

60   the posterior portion of the uropatagium in CAGS–Z070 (Fig. 1**o**–**p**). As reported

61   elsewhere, they are parallel to subparallel and closely packed. Individual fibres are

62   0.08–0.11 mm wide (ca. 5 fibres per mm) and at least 1.9 mm long. Pycnofibres are

63   preserved extensively in both pterosaur specimens (especially CAGS–Z070; Figs. 1

64 and 2, and Supplementary Figs. 1, 4 and 5) and are discriminated from structural

65 fibres based on their curved morphology and overlapping arrangement. In the

66 posterior portion of the uropatagium in CAGS–Z070, pycnofibres co-occur with

67 structural fibres; oblique intersections reflect superposition of these features during

68 decay (Fig. 1**o**–**p**).

69   Pycnofibres are categorized here into four types. Type 1 occurs around the head,

70 neck, shoulder, torso, all four limbs and tail of both specimens (Figs. 1**c**–**e**, **o**–**p**, 2**b**–**c**

71 and **f**). It comprises curved monofilaments that are 3.5–12.8 mm long and 70–430 μm

72 wide. Some short, distally tapering examples discriminate between dark-toned lateral

73 margins and light-toned axial regions, especially near the filament base where the

74 light-toned axis is wider, suggesting a tube-like morphology (Fig. 1**c**–**e**). Type 2 is

75 preserved in the neck, proximal forelimb, plantar metatarsus and proximal tail regions

76 of CAGS–Z070. It consists of bundles of curved filaments of similar length that

77 appear to form brush-like structures at the distal ends of thicker filaments (2.0–13.8

78 mm long and 80–180 μm wide) (Fig. 1**f**–**h**). The latter may represent individual thick

79 filaments or fused proximal regions of thinner distal filaments. Type 3 occurs around

80 the head of CAGS–Z070. It comprises straight to slightly curved, distally tapered,

81 central filaments (4.5–7.0 mm long and 50–450 μm wide) with short lateral branches

82 that diverge from the central filament near the midpoint (Fig. 1**i**–**k**). There are five

83 Type 3 filaments identified on the head, next to five similar filaments likely of the

84 same nature but obscured by overlapping filaments (Supplementary Fig. 5**b**). Type 4

85 occurs on the wing membrane of both specimens. It comprises tufts of curved

86 filaments (2.5–8.0 mm long and 70–130 μm wide) that diverge proximally (Figs. 1**l**–**n**

87 and 2**d**–**e**), in contrast to the clear separation between Type 1 filaments (Fig. 1**o**–**p**).

88   Filamentous integumentary structures in extant and fossil vertebrates commonly

89 contain melanin-bearing organelles (melanosomes). Scanning electron microscopy

90 (SEM) of the filamentous structures of NJU–57003 reveals densely packed

91 microbodies 0.70 ± 0.11 μm long and 0.32 ± 0.05 μm wide (Fig. 2**g**–**h**,

92 Supplementary Figs. 4**a**–**f**, 6 and 7, and Supplementary Table 2). As with most

93 melanosome-rich fossil feathers[19-21], energy dispersive X-ray spectroscopy (EDS)

94 spectra of the filaments are dominated by a major peak for carbon (Supplementary

95 Fig. 8). These carbonaceous microbodies resemble fossil melanosomes in terms of

96 their geometry, dense packing, parallel alignment relative to the long axis of the

97 integumentary structure (i.e. barbules in Paraves), and preservation within the matrix

98 of the filament (see Supplementary text). Most of the microbodies are oblate and

99 morphologically similar to those that are usually interpreted as phaeomelanosomes in

100 fossils[19] (Fig. 2**h**). Rod-shaped examples, usually interpreted as eumelanosomes in

101 fossils[19] (Fig. 2**g**), are rare.

102   Fourier transform infrared spectroscopy (FTIR) of samples of pterosaur filaments

103 shows four major peaks unique to the filaments (Fig. 2**i**). These peaks are consistent

104 with the absorption regions of amide I at ca. 1650 cm^{-1} (principally the C=O

105 asymmetric stretching vibration with some C–N bending), amide II at ca. 1540 cm^{-1}

106 (a combination of N–H in-plane bending and C–N and C–C stretching as in indole

107 and pyrrole in melanin and amino acids), and aliphatic C–H stretching at 2850 cm^{-1}

108 and 2918 cm^{-1} [22]. These peaks also occur in spectra obtained from extant feathers[21,23],

109 fossil feathers of the paravian *Anchiornis*[20], and melanosomes isolated from human

110 hair[24]. Further, spectra of the pterosaur filaments more closely resemble those of

111 pheomelanin-rich red human hair in the stronger absorption regions at ca. 2850 cm^{-1}

112 and 2918 cm^{-1} and higher resolution in the region ca. 1500–1700 cm^{-1} than those

113 from eumelanin-rich black human hair and the ink sac of cuttlefish[24]. This, together

114 with the SEM results, suggests that the densely packed microbodies in the pterosaur

115 filaments are preserved melanosomes. The amide I peak at 1650 cm^{-1} is more

116 consistent with α-keratin (characteristic of extant mammal hair[25]) than β-keratin (the

117 primary keratin in extant avian feathers[22,26]). This signal may be original or

118 diagenetic; the molecular configuration of keratin[26] and other proteins[27] can alter

119 under mechanical stress and changes in hydration levels.

120   The ultrastructural and chemical features of the pterosaur filaments confirm that

121 they are hair-like or feather-like integumentary structures. The four types of filaments

122 described here show distinct distributions and morphologies. They are separated

123 clearly from the sedimentary matrix by sharp boundaries (Supplementary Fig. 4**g**–**i**).

124 There is no evidence that one or more filament type(s) were generated

125 taphonomically, e.g. through selective degradation or fossilization, or superimposition

126 of filaments. For instance, although Type 1 and 4 filaments occur widely in both

127 specimens, Type 4 occurs only in the wings, while Type 1 occupies the remaining

128 body regions. Type 1 filaments are thus not degraded products of Type 4, and Type 4

129 filaments do not represent superimposed clusters of Type 1 filaments. Filament types

130   2 and 3 occur only in CAGS–Z070. Type 3 occurs only in the facial area and is

131   associated with Type 1, where Types 2 and 4 are not evident. Type 3 filaments are

132   thus not degraded Type 2 or 4 filaments. Central filaments of Type 3 are

133   morphologically identical to the short, distally tapering filaments of Type 1, but the

134   branching filaments are much thinner (< 40 μm (Type 3) versus >70 μm (Type 1)

135   wide) and shorter (< 0.6 mm vs. > 3.5 mm long) than the latter. The branching

136   filaments are thus unlikely to reflect superimposition of clusters of Type 1 filaments.

137   In contrast, the distal ends of Type 2 filaments are similar, and have a similar

138   distribution pattern to, Type 1 filaments. An alternative interpretation, that Type 2

139   filaments might represent superimposition of Type 1 filaments at their proximal ends,

140   is unlikely (see detailed discussion in Supplementary text).Feathers and feather-like

141   integumentary structures have been reported in non-avian dinosaurs, although debate

142   continues about their true nature[2]. These structures have been ascribed to several

143   morphotypes, some absent in living birds[3,5], and provide a basis to analyse the

144   evolutionary significance of pterosaur pycnofibres. The pterosaur Type 1 filaments

145   resemble monofilaments in the ornithischian dinosaurs *Tianyulong* and *Psittacosaurus*

146   and the coelurosaur *Beipiaosaurus*: unbranched, cylindrical structures with a midline

147   groove that widens towards the base (presumed in *Beipiaosaurus*)[3,5]. The pterosaur

148   Type 2 filaments resemble the brush-like bundles of filaments in the coelurosaurs

149   *Epidexipteryx* and *Yi*[3,5,28]: both comprise parallel filaments that unite proximally. The

150   morphology and circum-cranial distribution of pterosaur Type 3 filaments resemble

151   bristles in modern birds[1], but surprisingly do not correspond to any reported

152   morphotype in non-avian dinosaurs. The Type 3 filaments recall bilaterally branched

153   filaments in *Sinornithosaurus*, *Anchiornis*, and *Dilong*, but the latter filaments branch

154   throughout their length rather than halfway along the central filament(s), as in the

155   pterosaur structure[3,5]. The pterosaur Type 4 filaments are identical to the radially

156   branched, downy feather-like morphotype found widely in coelurosaurs such as

157   *Sinornithosaurus*, *Beipiaosaurus*, *Protarchaeopteryx*, *Caudipteryx*, and *Dilong*[3,5].

158   The filamentous integumentary structures in our anurognathid pterosaurs are thus

159   remarkably similar to feathers and feather-like structures in non-avian dinosaurs.

160   Intriguingly, cylindrical (Type 1), radially symmetrical branched (Types 2 and 4) and

161   bilaterally symmetrical branched (Type 3) filaments clearly coexisted in individual

162   animals; these structures may represent transitional forms in the evolution of feathers,

163   as revealed by developmental studies[3,5].These new findings warrant revision of the

164   origin of complex feather-like branching integumentary structures from Dinosauria to

165   Avemetatarsalia, the wider clade that includes dinosaurs, pterosaurs, and close

166   relatives[4,29]. The early evolutionary history of bird feathers and homologous structures

167   in dinosaurs, and the multiple complex pycnofibres of pterosaurs, is enigmatic. A

168   previous study concluded that the common ancestor of these clades bore scales and

169   not filamentous integumentary appendages[2], but this result emerged only when the

170   filaments of pterosaurs were coded as non-homologous with those of dinosaurs. There

171   are no morphological criteria, however, for such a determination. The presence of

172   multiple pycnofibre types and their morphological, ultrastructural and chemical

173   similarity to feathers and feather-like structures in various dinosaurian clades,

174 confirms their likely homology with filamentous structures in non-avian dinosaurs

175 and birds. Comparative phylogenetic analysis produces equivocal results: maximum

176 likelihood modelling of plausible ancestral states, against various combinations of

177 branch length and character transition models (Supplementary text and

178 Supplementary Fig. 9, Table 3), reveals various potential solutions. The statistically

179 most likely result (Fig. 3 and Supplementary Table 3, highest log-likelihood value)

180 shows that the avemetatarsalian ancestors of dinosaurs and pterosaurs possessed

181 integumentary filaments, with highest likelihood of possessing monofilaments; tufts

182 of filaments, and, especially, brush-type filaments, are less likely ancestral states. This

183 confirms that feather-like structures arose in the Early or Middle Triassic. The

184 alternative tree for Dinosauria, with Ornithischia and Theropoda paired as

185 Ornithoscelida[30], produces an identical result.

186   We present these modelling data with caution, however, for two reasons: (1) the

187 tree rooting method can influence the result (Supplementary Table 3), favouring

188 results in which either scales are the basal condition or where non-theropod feather-

189 like structures and feathers evolved independently (Supplementary Figure 9, Table 3),

190 and (2) there is no adequate way to model probabilities of evolution of all six feather

191 types, or to model probabilities of transitions between the six different feather types.

192   The discovery of multiple types of feather-like structures in pterosaurs has broad

193 implications for our understanding of pterosaur biology and the functional origin of

194 feather-like structures in Avemetatarsalia[31,32]. Potential functions of these structures

195 include insulation, tactile sensing, streamlining and coloration (primarily for

196 camouflage and signalling), as for bristles, down feathers and mammalian hairs[31-34].

197 Type 1, 2 and 4 filaments could shape a filamentous covering around the body and

198 wings (Fig. 4) that might have functioned in streamlining the body surface in order to

199 reduce drag during flight, as for modern bat fur or avian covert feathers[33,35]. Type 1

200 and 2 filaments occur in considerably high densities, particularly around the neck,

201 shoulder, hindlimb and tail regions where the high degree of superposition prevents

202 easy discrimination of adjacent fibres. This, along with the wide distribution and

203 frayed appearance, resembles mammalian underfur adapted for thermal insulation[36,35].

204 Despite the less dense packing of Type 4 filaments on the wings, the morphology of

205 the structures is consistent with a thermoregulatory function: down feathers can

206 achieve similar insulation as mammalian hair with only about half the mass, due to

207 their air-trapping properties and high mechanical resilience, effective in retaining an

208 insulating layer of still air[38]. This may optimize the encumbrance of the large wing

209 area to wing locomotion[18]. Type 3 filaments around the jaw (Fig. 4) may have had

210 tactile functions in e.g. prey handling, information gathering during flight, navigating

211 in nest cavities and on the ground at night, similar to bristles in birds[39].
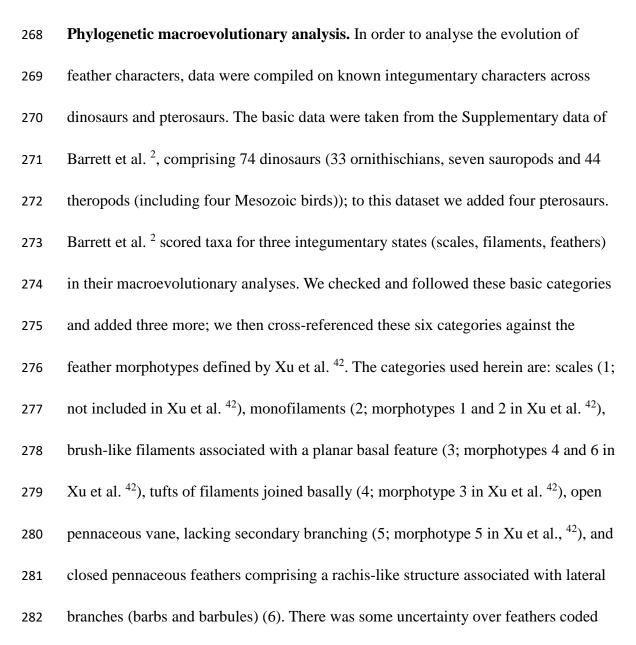
212

213 **Methods**

214 **Sampling.** The specimen NJU–57003 is represented by two fragmented slabs, both

215 containing original bone, fossilized soft tissues, and natural moulds of bones. Each

216 slab was glued together along the fissures by fossil dealers with the fossil on the

217   surfaces untouched. The specimen CAGS–Z070 is represented by a single unbroken

218   slab. Small flakes (1–3 mm wide) of samples with preserved integument and/or

219   enclosing sediments were carefully removed from the inferred integumentary

220   filaments from different parts of NJU–57003 (Supplementary Figs. 1**a** and 4**a**–**c**)

221   using a dissecting scalpel. This method was used to avoid sampling from degraded

222   products of other tissues, such as dermis, epidermis, or even internal organs. Most

223   samples were not treated further; the remainder were sputter-coated with Au to

224   enhance SEM resolution (Fig. 2**g**–**h** and Supplementary Figs. 4**a**–**f** and 6). All

225   experiments described below were repeated in order to validate the results.

226

227   **SEM.** Samples were examined using a JEOL 8530F Hyperprobe at the School of

228   Earth Sciences, University of Bristol, and a LEO 1530VP scanning electron

229   microscope at the Technical Services Centre, Nanjing Institute of Geology and

230   Palaeontology, Chinese Academy of Sciences. Both instruments were equipped with a

231   secondary electron (SE) detector, a back-scattered electron (BSE) detector and an

232   energy dispersive X-ray spectrometer (EDS).

233

234   **Measurements of melanosomes.** The geometry of melanosomes was measured from

235   SEM images using the image-processing program ImageJ (available for download at

236   http://rsbweb.nih.gov/ij/). We measured maximum short and long axis length of

237   melanosomes that were oriented perpendicular to line of sight, and from these data we

238   calculated mean and coefficient of variation (CV) of the long and short axis, and mean

239   aspect ratio (long:short axis). Based on the proposed taphonomic alteration of fossil

240   melanosome size (shrinkage up to ~20% in both length and diameter)[40,41], we

241   modelled potential diagenetic alteration by enlarging original measurements by 20%.

242

243   **FTIR microspectroscopy.** Samples of the filamentous tissues and the associated

244   sediments were removed separately from NJU–57003 and placed on a BaF_2 plate

245   without further treatment. The IR absorbance spectra were collected using a Thermo

246   iN10MX infrared microscope with a cooled MCT detector, at the School of Earth

247   Sciences, University of Bristol. The microscope was operated in transmission mode

248   with a 15x15 micron aperture. 10 spectra were obtained from the filamentous tissues.

249   The spectra show consistent results and the example presented in Fig. 2 shows the

250   highest signal to noise ratio and was obtained with 2 cm^{-1} resolution and 2000 scans.

251

252   **Fluorescence microscopy.** Selected areas with extensive soft tissue preservation in

253   NJU–57003 were investigated and photographed using a Zeiss Axio Imager Z2

254   microscope with a digital camera (AxioCam HRc) and a fluorescence illuminator

255   (514 nm LED) attached, at the Technical Services Centre, Nanjing Institute of

256   Geology and Palaeontology, Chinese Academy of Sciences.

257

258   **Laser-stimulated fluorescence (LSF) imaging and data reduction protocol.** LSF

259   images were collected using the protocol of Kaye et al. [15,16]. NJU–57003 was imaged

260   with a 405 nm 500 mw laser that was projected into a vertical line by a Laserline

261 Optics Canada lens. The laser line was swept repeatedly over the specimen during the

262 exposure time for each image in a dark room. Images were captured with a Nikon

263 D610 DSLR camera fitted with an appropriate long pass blocking filter in front of the

264 lens to prevent image saturation by the laser. Standard laser safety protocols were

265 followed during laser usage. The images were post processed in Photoshop CS6 for

266 sharpness, colour balance and saturation.

267

268 **Phylogenetic macroevolutionary analysis.** In order to analyse the evolution of

269 feather characters, data were compiled on known integumentary characters across

270 dinosaurs and pterosaurs. The basic data were taken from the Supplementary data of

271 Barrett et al. [2], comprising 74 dinosaurs (33 ornithischians, seven sauropods and 44

272 theropods (including four Mesozoic birds)); to this dataset we added four pterosaurs.

273 Barrett et al. [2] scored taxa for three integumentary states (scales, filaments, feathers)

274 in their macroevolutionary analyses. We checked and followed these basic categories

275 and added three more; we then cross-referenced these six categories against the

276 feather morphotypes defined by Xu et al. [42]. The categories used herein are: scales (1;

277 not included in Xu et al. [42]), monofilaments (2; morphotypes 1 and 2 in Xu et al. [42]),

278 brush-like filaments associated with a planar basal feature (3; morphotypes 4 and 6 in

279 Xu et al. [42]), tufts of filaments joined basally (4; morphotype 3 in Xu et al. [42]), open

280 pennaceous vane, lacking secondary branching (5; morphotype 5 in Xu et al., [42]), and

281 closed pennaceous feathers comprising a rachis-like structure associated with lateral

282 branches (barbs and barbules) (6). There was some uncertainty over feathers coded

283   herein as type 3, which could correspond to morphotype 6, or morphotypes 4 and 6 in

284   Xu et al. [42]. However, the only taxa coded with these as the most derived feather type

285   are *Sordes pilosus* and *Beipiaosaurus inexpectus*. These taxa belong to separate clades

286   and thus the calculation of ancestral states is not affected by how our feather type 3 is

287   coded (i.e. whether treating morphotypes 4 and 6 of Xu et al. [42] in combination or

288   separately).

289   As in previous studies[2], we used maximum-likelihood (ML) approaches to

290   explore trait evolution. There are many methods to estimate ancestral states for

291   continuous characters, but choices are more limited for discrete characters, such as

292   here, where only ML estimation of ancestral states is appropriate[43]. We calculated ML

293   reconstructions of ancestral character states using the 'ace' function of the ape R

294   package[44], with tree branch lengths estimated in terms of time, derived using the

295   'timePaleoPhy' function in the paleotree package[45] and the 'DatePhylo' function in

296   the strap R package[46]. These enabled us to assess results according to three methods

297   of estimating branch lengths, the 'basic' method, which makes each internal node in a

298   tree the age of its oldest descendant, the 'equal branch length' (equal) method, which

299   adds a pre-determined branch length (often 1 Myr) to the tree root and then evenly

300   distributes zero-length branches at the base of the tree, and the 'minimum branch

301   length' (mbl) method, which minimizes inferred branching times and closely

302   resembles the raw, time-calibrated tree. A problem with the 'basic' branch length

303   estimation is that it results in many branch lengths of length zero, in cases where

304   many related taxa are of the same age; in these cases, we added a line of code to make

305   such zero branch lengths equal to 1/1000000 of the total tree length. A criticism of the

306   mbl method is that it tends to extend terminal branching events back in time,

307   especially when internal ghost lineages are extensive[2], but this is not the case here,

308   and the base of the tree barely extends to the Triassic / Jurassic boundary.

309   We ran our analyses using three evolutionary models with different rates of

310   transition between the specified number of character states (six here), namely "ER",

311   an equal-rates model, "ARD", an all-rates-different model and "SYM", a symmetrical

312   model. These were calculated using the 'ace' function in ape[2] and the

313   'add.simmap.legend' function of the R package 'phytools' [47].

314   In a further series of analyses, we attempted to model the macroevolution of all

315   traits, as coded (see Supplementary results), so coding multiple trait values for taxa

316   that preserve multiple feather types. This did not shed much light on patterns of

317   evolution of feather types because the multiple trait codings (e.g. 1,2 or 2,5,6) were

318   each made into a new state, making 14 in all, and these were not linked. Therefore,

319   the six multiply coded taxa that each had feather type 6 were represented as six

320   independent states and their evolution tracked in those terms. Further, we attempted to

321   separate the six characters, so they would track through the tree, whether recorded as

322   singles or multiples in different taxa; however, we did not have the information to

323   enable us to do this with confidence because of gaps in coding. In terms of reality,

324   these multiply coded taxa still represent an incomplete sample of the true presence

325   and absence of character states - by chance, many coelurosaurs are not coded for

326   scales (1) or monofilaments (1), and yet it is likely they all had these epidermal

327 appendages. Therefore, attempting to run such multiple codings, with characters

328 either as groups or coded independently, encounters so many gaps that the result is

329 hard to interpret. Our approach is to code the most derived feather in each taxon, and

330 that too is incomplete because of fossilization gaps, but at least it represents a

331 minimal, or conservative, approach to trait coding and hence to the discoveries of

332 macroevolutionary patterns of feather evolution; complete fossil data might show

333 wider distributions of each feather type and hence deeper hypothesized points of

334 origin. Complete coding of feather types would of course allow each trait to be

335 tracked in a multiple-traits analysis.

336

337 **Data availability**

338 The data that support the findings of this study are available from the corresponding

339 authors upon reasonable request.

340

341 **References**

342   1   Lucas, A. M. S. & Peter, R. *Avian anatomy: integument* (U.S. Agricultural

343   Research Service, Washington, 1972).

344   2   Barrett, P. M., Evans, D. C. & Campione, N. E. Evolution of dinosaur epidermal

345   structures. *Biol. Lett.* **11**, 20150229 (2015).

346   3   Xu, X. *et al.* An integrative approach to understanding bird origins. *Science* **346**,

347   1253293 (2014).

348 4   Di-Poï, N. & Milinkovitch, M. C. The anatomical placode in reptile scale

349   morphogenesis indicates shared ancestry among skin appendages in amniotes.

350   *Sci. Adv.* **2**, e1600708 (2016).

351 5   Chen, C. F. *et al.* Development, regeneration, and evolution of feathers. *Ann. Rev.*

352   *Anim. Biosci.* **3**, 169–195 (2015).

353 6   Mayr, G., Pittman, M., Saitta, E., Kaye, T. G. & Vinther, J. Structure and

354   homology of *Psittacosaurus* tail bristles. *Palaeontol.* **59**, 793–802 (2016).

355 7   Zheng, X. T., You, H. L., Xu, X. & Dong, Z. M. An Early Cretaceous

356   heterodontosaurid dinosaur with filamentous integumentary structures. *Nature*

357   **458**, 333–336 (2009).

358 8   Godefroit, P. *et al.* A Jurassic ornithischian dinosaur from Siberia with both

359   feathers and scales. *Science* **345**, 451–455 (2014).

360 9   Kellner, A. W. *et al.* The soft tissue of *Jeholopterus* (Pterosauria, Anurognathidae,

361   Batrachognathinae) and the structure of the pterosaur wing membrane. *Proc. Biol.*

362   *Sci.* **277**, 321–329 (2010).

363 10   Sharov, A. G. New flying reptiles from the Mesozoic of Kazakhstan and Kirgizia

364   (in Russian). *Akad. nauk SSSR Paleont. Inst. Tr.* **130**, 104–113 (1971).

365 11   Czerkas, S. A. & Ji, Q. A new rhamphorhynchoid with a headcrest and complex

366   integumentary structures. In: S. J. CZERKAS (Ed), Feathered dinosaurs and the

367   origin of flight (Blanding, The Dinosaur Museum), 15–41 (2002).

368 12   Unwin, D. M. & Bakhurina, N. N. *Sordes pilosus* and the nature of the pterosaur

369   flight apparatus. *Nature* **371**, 62–64 (1994).

370   13 Ji, Q. & Yuan, C. Discovery of two kinds of protofeathered pterosaurs in the

371   Mesozoic Daohugou Biota in the Ningcheng region and its stratigraphic and

372   biologic significances. *Geol. Rev.* **48**, 221–224 (2002).

373   14 Xu, X., Zhou, Z., Sullivan, C., Wang, Y. & Ren, D. An updated review of the

374   Middle-Late Jurassic Yanliao Biota: chronology, taphonomy, paleontology and

375   paleoecology. *Acta Geol. Sin. (Engl. Ed.)* **90**, 2229–2243 (2016).

376   15 Wang, X. *et al.* Basal paravian functional anatomy illuminated by high-detail

377   body outline. *Nat. Commun.* **8,** (2017).

378   16 Kaye, T. G. *et al.* Laser-stimulated fluorescence in paleontology. *PloS one* **10**,

379   e0125923 (2015).

380   17 Unwin, D. M. On the phylogeny and evolutionary history of pterosaurs. *Geol.*

381   *Soc., London, Spec. Publ.* **217**, 139–190 (2003).

382   18 Frey, E., Tischlinger, H., Buchy, M. C., & Martill, D. M. New specimens of

383   Pterosauria (Reptilia) with soft parts with implications for pterosaurian anatomy

384   and locomotion. *Geol. Soc., London, Spec. Publ.* **217**, 233–266 (2003).

385   19 Lindgren, J. *et al.* Interpreting melanin-based coloration through deep time: a

386   critical review. *Proc. R. Soc. B* **282**, 20150614 (2015).

387   20 Lindgren, J. *et al.* Molecular composition and ultrastructure of Jurassic paravian

388   feathers. *Sci. Rep.* **5**, 13520 (2015).

389   21 Barden, H. E. *et al.* Morphological and geochemical evidence of eumelanin

390   preservation in the feathers of the Early Cretaceous bird, *Gansus yumenensis*.

391   *PLoS One* **6**, e25494 (2011).

392   22 Bendit, E. Infrared absorption spectrum of keratin. I. Spectra of α-, β-, and

393   supercontracted keratin. *Biopolymers* **4**, 539–559 (1966).

394   23 Martinez-Hernandez, A. L., Velasco-Santos, C., De Icaza, M. & Castano, V. M.

395   Microstructural characterisation of keratin fibres from chicken feathers. *Int. J.*

396   *Envir. Pollut.* **23**, 162–178 (2005).

397   24 Liu, Y. *et al.* Comparison of structural and chemical properties of black and red

398   human hair melanosomes. *Photochem. Photobiol.* **81**, 135–144 (2005).

399   25 Alibardi, L. Adaptation to the land: the skin of reptiles in comparison to that of

400   amphibians and endotherm amniotes. *J. Exp. Zool.* **298B,** 12–41 (2009).

401   26 Kreplak, L., Doucet, J., Dumas, P. & Briki, F. New aspects of the α-helix to β-

402   sheet transition in stretched hard α-keratin fibers. *Biophys. J.* **87**, 640–647 (2004).

403   27 Yassine, W., Taib, N., Federman, S., Milochau, A., Castano, S., Sbi, W.

404   Manigand, C., Laguerre, M., Desbat, B., Oda, R. & Lang, J. Reversible transition

405   between α-helix and β-sheet conformation of a transmembrane domain. *Biochim.*

406   *Biophys. Acta – Biomembranes.* **1788**, 1722–1730 (2009).

407   28 Xu, X. *et al.* A bizarre Jurassic maniraptoran theropod with preserved evidence of

408   membranous wings. *Nature* **521**, 70–73 (2015).

409   29 Donoghue, P. C. J. & Benton, M. J. Rocks and clocks: calibrating the Tree of Life

410   using fossils and molecules. *Trends Ecol. Evol.* **22**, 424–431 (2007).

411   30 Baron, M. G., Norman, D. B. & Barrett, P. M. A new hypothesis of dinosaur

412   relationships and early dinosaur evolution. *Nature* **543**, 501–506 (2017).

413   31 Persons IV, W. S. & Currie, P. J. Bristles before down: a new perspective on the

414   functional origin of feathers. *Evolution* **69**, 857–862 (2015).

415   32 Ruxton, G. D., Persons IV, W. S. & Currie, P. J. A continued role for signaling

416   functions in the early evolution of feathers. *Evolution* **71**, 797–799 (2017).

417   33 Bullen, R. D. & McKenzie, N. L. The pelage of bats (Chiroptera) and the

418   presence of aerodynamic riblets: the effect on aerodynamic cleanliness. *Zoology*

419   **111**, 279–286 (2008).

420   34 Caro, T. The adaptive significance of coloration in mammals. *BioScience* **55**,

421   125–136 (2005).

422   35 Homberger, D. G., & de Silva, K. N. Functional microanatomy of the feather-

423   bearing integument: implications for the evolution of birds and avian flight. *Amer.*

424   *Zool.* **40**, 553–574 (2000).

425   36 Scholander, P., Walters, V., Hock, R. & Irving, L. Body insulation of some arctic

426   and tropical mammals and birds. *Biol. Bull.* **99**, 225–236 (1950).

427   37 Ling, J. K. Pelage and molting in wild mammals with special reference to aquatic

428   forms. *Quart. Rev. Biol.* **45**, 16–54 (1970).

429   38 Gao, J., Yu, W. & Pan, N. Structures and properties of the goose down as a

430   material for thermal insulation. *Text. Res. J.* **77**, 617–626 (2007).

431   39 Cunningham, S. J., Alley, M. R., & Castro, I. Facial bristle feather histology and

432   morphology in New Zealand birds: implications for function. *J. Morphol.* **272**,

433   118–128 (2011).

434   40 McNamara, M. E., Briggs, D. E. G., Orr, P. J., Field, D. J. & Wang, Z.

435   Experimental maturation of feathers: implications for reconstructions of fossil

436   feather colour. *Biol. Lett.* 9, 20130184 (2013).

437   41   Colleary C, Dolocan A, Gardner J, *et al.* Chemical, experimental, and

438   morphological evidence for diagenetically altered melanin in exceptionally

439   preserved fossils. *Proc. Natl. Acad. Sci.* **112,** 12592–12597 (2015).

440   42   Xu, X., Zheng, X. & You, H. Exceptional dinosaur fossils show ontogenetic

441   development of early feathers. *Nature* **464**, 1338–1341 (2010).

442   43   Pagel, M. Detecting correlated evolution on phylogenies: a general method for

443   the comparative analysis of discrete characters. *Proc. R. Soc. Lond. B* **255**, 37–45

444   (1994).

445   44   Paradis, E. *Analysis of Phylogenetics and Evolution with R*. (Springer Science &

446   Business Media, 2011).

447   45   Bapst, D. W. paleotree: paleontological and phylogenetic analyses of evolution. v.

448   2.3. See https://github.com/dwbapst/paleotree (2015).

449   46   Bell, M. A. & Lloyd, G. T. Strap: an R package for plotting phylogenies against

450   stratigraphy and assessing their stratigraphic congruence. *Palaeontol.* **58**, 379–

451   389 (2015).

452   47   Revell, L. J. phytools: an R package for phylogenetic comparative biology (and

453   other things). *Methods Ecol. Evol.* **3**, 217–223 (2012).

454

455   **Supplementary Information** is available in the online version of the paper.

456

457 **Acknowledgements**

466

467 **Author Contributions**

468 B.Y.J. and M.J.B. designed the research, Z.X.Y., B.Y.J. and X.X. systematically

469 studied the specimens, Z.X.Y., S.L.K., M.E.M, and P.J.O. did the SEM analysis,

470 Z.X.Y. and B.Y.J. did the FTIR analysis, M.P. and T.G.K. did the LSF imaging, data

471 reduction and interpretation, M.J.B. did the maximum likelihood analyses, and

472 Z.X.Y., B.Y.J., M.J.B., M.E.M, X.X. and P.J.O. wrote the paper; all authors approved

473 the final draft of the paper.

474

475 **Author Information**

476 Reprints and permissions information is available at www.nature.com/reprints. The

477 authors declare no competing financial interests. Correspondence and requests for

478 materials should be addressed to B.Y.J. (byjiang@nju.edu.cn) or M.J.B.

479 (mike.benton@bristol.ac.uk).

480

481 **Figure 1 | Integumentary filamentous structures in CAGS–Z070. a**, Overview

482 shows extensive preservation of soft tissues. **b–p**, Details of the integumentary

483 filaments in the regions indicated in **a** on the head and neck (**b–d**, **i–j**), forelimb (**f–g**),

484 wing (**l–m**) and tail (**o–p**), and illustrated reconstructions of the filaments (**e**: Type 1

485 filament; **h**: Type 2 filament; **k**: Type 3 filament; **n**: Type 4 filament). Scale bars: 20

486 mm in **a**; 10 mm in **b**; 500 µm in **c** and **i**; 100 µm in **d**; 1 mm in **f**, **l**, **m** and **p**; 200 µm

487 in **g** and **j**; 5 mm in **o**.

488

489 **Figure 2 | Preservation, microstructure and chemistry of the integumentary**

490 **filamentous structures in NJU–57003. a**, Laser-stimulated fluorescence[6,15,16] image

491 highlights extensive preservation of soft tissues (black areas). **b–f**, Details of the

492 integumentary filaments in the regions indicated in A on the head and neck (**b–c**),

493 wing (**d–e**) and tail (**f**). **g–h**, Scanning electron micrographs of the monofilaments on

494 the neck and hindlimb of NJU–57003 (samples 10 and 39, respectively,

495 Supplementary Fig. 1**a**) show densely packed, elongate and oblate melanosomes. **i**,

496 FTIR absorbance spectra of the monofilaments, monofilaments with sediment matrix,

497 and sediment matrix in NJU–57003 (Sample 15, Supplementary Fig. 1**a**) compared

498 with spectra from a feather of *Anchiornis* (from ref. [20]), extant Marabou stork feather

499   (from ref. [21]) and black and red human hair melanosomes (from ref. [24]). Scale bars: 20

500   mm in **a**; 1 mm in **b**, **c** and **e**; 5 mm in **d** and **f**; 1 μm in **g** and **h**.

501

502   **Figure 3 | Phylogenetic comparative analysis of integumentary filament and**

503   **feather evolution in pterosaurs and archosaurs.** The phylogeny is scaled to

504   geological time, with recorded terminal character states for each species, and

505   estimated ancestral character states at the lower nodes. The model is the most likely of

506   the maximum likelihood models, based on minimum-branch lengths (mbl) and

507   transitions occurring as all-rates-different (ARD), but other results with lower

508   likelihoods show scales as ancestral. The ancestral state reconstruction shows a

509   combination of monofilaments, tuft-like filaments, and brush-type filaments as the

510   ancestral state for Avemetatarsalia and for Dinosauria. The estimated ancestral state

511   for Theropoda comprises all five feather states. Numbered small vertical arrows

512   indicate earliest occurrences of feather types 2–6. Two hypotheses for timing of avian

513   feather origins are indicated: A, early origin, at the base of Avemetatarsalia in the

514   Early Triassic, or B, late origin, at the base of Maniraptora in the Early–Middle

515   Jurassic.

516

517   **Figure 4 | Reconstruction of one of the studied anurognathid pterosaurs, exhibiting**

518   **diverse types of pycnofibres distributed in different body parts.**